
Article:
Woodhouse, Shannon, He, Zhesi orcid.org/0000-0001-8335-9876, Woolfenden, Hugh et al. (6 more authors) (2021) Validation of a novel associative transcriptomics pipeline in Brassica oleracea: Identifying candidates for vernalisation response. BMC Genomics. 539. ISSN 1471-2164

https://doi.org/10.1186/s12864-021-07805-w

Validation of a novel associative transcriptomics pipeline in *Brassica oleracea:* Identifying candidates for vernalisation response

Shannon Woodhouse[1], Zhesi He[2], Hugh Woolfenden[3], Burkhard Steuernagel[3], Wilfried Haerty[4,5], Ian Bancroft[2], Judith A. Irwin[1], Richard J. Morris[3*], Rachel Wells[1*]

[1]Department of Crop Genetics, John Innes Centre, NR47UH Norwich, UK. [2]Department of Biology, University of York, Heslington, YO105DD York, UK. [3]Computational & Systems Biology, John Innes Centre, NR47UH Norwich, UK. [4]Earlham Institute, NR47UH Norwich, UK. [5]School of Biological Sciences, University of East Anglia, NR47TJ Norwich, UK

*email: richard.morris@jic.ac.uk, rachel.wells@jic.ac.uk

Abstract

Background: Associative transcriptomics has been used extensively in *Brassica napus* to enable the rapid identification of markers correlated with traits of interest. However, within the important vegetable crop species, *Brassica oleracea,* the use of associative transcriptomics has been limited due to a lack of fixed genetic resources and the difficulties in generating material due to self-incompatibility. Within Brassica vegetables, the harvestable product can be vegetative or floral tissues and therefore synchronisation of the floral transition is an important goal for growers and breeders. Vernalisation is known to be a key determinant of the floral transition, yet how different vernalisation treatments influence flowering in *B. oleracea* is not well understood.

Results: Here, we present results from phenotyping a diverse set of 69 *B. oleracea* accessions for heading and flowering traits under different environmental conditions. We developed a new associative transcriptomics pipeline, and inferred and validated a population structure, for the phenotyped accessions. A genome-wide association study identified miR172D as a candidate for the vernalisation response. Gene expression marker association identified variation in expression of *BoFLC.*C2 as a further candidate for vernalisation response.

Conclusions: This study describes a new pipeline for performing associative transcriptomics studies in *B. oleracea*. Using flowering time as an example trait, it provides insights into the genetic basis of vernalisation response in *B. oleracea* through associative transcriptomics and confirms its characterisation as a complex G x E trait. Candidate leads were identified in miR172D and *BoFLC.C2*. These results could facilitate marker-based breeding efforts to produce *B. oleracea* lines with more synchronous heading dates, potentially leading to improved yields.

Keywords

Associative Transcriptomics, GWAS, Population Structure, *Brassica oleracea,* Flowering, Vernalisation.

Introduction

Ensuring synchronous transiting from the vegetative to the reproductive phase is important for maximising the harvestable produce from brassica vegetables. Many cultivated brassica vegetables arose from their native wild form *B. oleracea* var. *oleracea* [1]. Wild cabbage, *B. oleracea* L., is a cruciferous perennial growing naturally along the coastlines of Western Europe. From this single species, selective breeding efforts have enabled the production of the numerous subspecies we see today. The specialization of a variety of plant organs has given rise to the large diversity seen within the species. Various parts of brassicas are harvested, including leaves (e.g. leafy-kale and cabbage), stems (e.g. kohl-rabi), and inflorescences (broccoli and cauliflower). For all subspecies, the shift from the vegetative to reproductive phase is important and being able to genetically manipulate this transition will aid the development and production of synchronous brassica vegetables.

Determining how both environmental and genotypic variation affect flowering time is important for unravelling the mechanisms behind this transition. For many *B. oleracea* varieties, a period of cold exposure, known as vernalisation, is required for the vegetative-to-floral transition to take place. This requirement for vernalisation, or lack thereof, determines whether the plant is a winter annual, perennial or biennial or whether it is rapid-cycling or a summer annual [2]. As a consequence, the response of the plant to vernalisation provides quantifiable variation that

has been exploited by breeders to develop varieties with more synchronous heading. Such variation will be key for future breeding in the face of a changing climate.

Genome-wide association studies (GWAS) are an effective means of identifying candidate genes for target traits from panels of genetically diverse lines [3]. GWAS has been used successfully in numerous plant species including Arabidopsis, maize, rice and Brassica [4–7]. However, its application is reliant on genomic resources which are not always available for complex polyploid crops. Associative transcriptomics uses the sequences of expressed genes (mRNAseq) aligned to a reference to identify and score molecular markers that correlate with trait data. These molecular markers represent variation in gene sequences and expression levels. Therefore, unlike traditional GWAS analysis, associative transcriptomics also enables identification of associations between traits and gene expression levels [4]. Associative transcriptomics is a robust method for identifying significant associations and is being used increasingly to identify molecular markers linked to trait-controlling loci in crops [8–11].

An important factor to account for in association studies is the genetic linkage between loci. If the frequency of association between the different alleles of a locus is higher or lower than what would be expected if the loci were independent and randomly assorted, then the loci are said to be in linkage disequilibrium (LD) [12]. LD will vary across the genome and across chromosomes and it is important to account for this in GWAS analyses. This variation in LD is due to many factors, including selection, mutation rate and genetic drift. Strong selection or admixture within a population will increase LD. Accounting for the correct population structure reduces the risk of detecting spurious associations within GWAS analyses. The population structure can be determined from unlinked markers [13].

Here, we develop and validate an associative transcriptomics pipeline for *B. oleracea.* A specific population structure consisting of unlinked markers was generated using SNP data from 69 lines of genetically fixed *B. oleracea* from the Diversity Fixed Foundation Set [14]. The

pipeline was successfully used for the identification of candidate leads involved in vernalisation response, identifying a strong candidate in miR172D.

Results

Exposure to different environmental conditions identifies vernalisation requirements across the phenotyped accessions

We selected a subset of 69 *B. oleracea* lines, diverse in both eco-geographic origin and crop type, from the *B. oleracea* Diversity Fixed Foundation Set [14]. We used these accessions to evaluate the importance of vernalisation parameters by quantifying flowering time under different conditions (vernalisation start, duration and temperature). Two key developmental stages were monitored: 'days to buds visible' (DTB) and 'days to first flower' (DTF). The variation in flowering time across the different treatments and between the different lines is shown in Fig. 1. The different vernalisation start times demonstrate that exposure to the longer, ten-week pre-vernalisation growth period (10WPG) typically results in earlier flowering, compared to the shorter, six-week pre-growth period (6WPG). The mean DTB for 6WPG was 21.0 days (SD = 51.6), compared to 5.8 days (SD = 49.9) for the 10WPG (Wilcoxon Test, W = 17958, P = 0.004). Similarly, we found a significant difference in the time taken to reach DTF between the two treatment groups, with a mean of 57.9 days (SD = 55.5) following the 6WPG, in comparison to 35.9 days (SD = 53.1) following the 10WPG (Wilcoxon Test, W = 17471, P = 2.96e-05).

Changes in vernalisation duration led to a significant difference in DTB, but not in DTF. Following the six-week vernalisation (6WV), the mean DTB was 9.5 days (SD = 44.5) compared to 5.8 days (SD = 46.8) after exposure to twelve-weeks of vernalisation (12WV) (Wilcoxon Test, W = 19532, P = 0.002). This difference was coupled with more synchronous

117 heading between lines following the 12WV period. The impact of vernalisation duration on
118 DTB varied across the population, reflecting the numerous factors that can affect DTB
119 depending on crop type, such as stem elongation and developmental arrest.

120 Of the three parameters we investigated, vernalisation temperature resulted in the most
121 pronounced phenotypic differences. The 5ºC vernalisation (5 ºCV) resulted in the largest DTB
122 (slowest overall bud development), whereas the 10ºC vernalisation (10 ºCV) treatment
123 resulted in the largest DTF. The distribution between heading dates was distinctly different
124 between the temperatures. Higher vernalisation temperatures resulted in larger the variation
125 in DTB and DTF. The more synchronous heading and flowering for the 5ºCV treatment
126 suggests that this temperature was able to saturate the vernalisation requirement for a large
127 proportion of the lines. After exposure to the warmer temperatures, the variation in DTB and
128 DTF were greatly increased (Additional File 1), indicating that the cooler vernalisation
129 temperature aided faster transitioning in some lines, but delayed the development of others.
130 This is consistent with differences in *B. oleracea* crop types, for example Brussels Sprouts are
131 known to have a strong vernalisation requirement, whereas Summer Cauliflower have been
132 bred to produce curd rapidly without the need for cold exposure [15,16].

133 The effect of vernalisation temperature on the floral transition is demonstrated clearly between
134 the Broccoli Mar DH and the Brussel Sprout Cavolo Di Bruxelles Precoce (Fig.1A), with polar
135 responses to vernalisation temperature. Mar DH transitioned fastest under the 15 ºC
136 vernalisation (15 ºCV) treatment, whereas Cavolo Di Bruxelles Precoce transitioned faster
137 under the 5 ºCV treatment. Faster transitions at higher vernalisation temperatures as in the
138 case of Mar DH, however, can lead to undesirable phenotypes from a grower's perspective
139 (Fig. 1B).

140

Unlinked markers are required to generate a representative population structure

GWAS requires trait, SNP and population data. The correct population structure is important for ensuring that associations are with the trait of interest rather than identified on account of relatedness within the population, in particular for panels of only one species. To generate a representative population structure, it is necessary to ensure the SNPs used are unlinked [13]. However, different criteria have been used to select these SNPs [6,17–19]. To evaluate the impact of SNP selection criteria, we generated two population structures and investigated their suitability for representing the panel.

Using all markers with a minor allele frequency (MAF) larger than 0.05 [4,20,21], reduced the total number of SNPs from 110,555 to 36,631. Calculation of ΔK showed a maximum value of K=2, although a further peak in ΔK was observed at K=5 (Additional File 6A), thus identifying substructure within the population. ΔK frequently identifies K=2 as the top level of hierarchical structure, even when more subpopulations are present [21,22]. Subsequent phylogenetic analysis (Additional File 7A, 7B) identified clusters representing these sub populations. Therefore, to account for substructure within the population, the value of K=5 was used for further analysis [22,23]. A second population structure was generated using stricter parameters, requiring the markers be biallelic, MAF > 0.05, one per gene and at least 500 bp apart. A total of 664 SNPs met these requirements, resulting in the identification of four subpopulation clusters (Additional File 4).

We assessed the two population structures based on crop type and phenotypic data. Using K=5, generated using the less stringent parameters, (Figs. 2A, 2C, 2E) cluster one contained only broccoli and calabrese, both members of the same subspecies var. *italica* [24,25], whereas cluster two mainly comprised cauliflower, subspecies var. *botrytis*. Late flowering accessions were included in both clusters. Interestingly, this population structure grouped the

rapid cycling and late flowering kales together with a spread of accessions from other crop types, in cluster four. The remaining two clusters were small by comparison: cluster three comprised of seven accessions, a mixture of broccoli, cauliflower and kale; cluster five consisted of just two lines, one kale and one cauliflower.

The four clusters identified using more stringent SNP selection criteria contained all of the rapid cycling kales in cluster one, characterised by their early heading and flowering phenotypes (Figs. 2B, 2D, 2F). This was identified as a clear subgroup within the phylogenetic tree (Additional File 7C). Cluster two was mainly broccoli and calabrese, whilst cluster three consisted largely of the earlier flowering cauliflowers. Cluster four contained the late flowering individuals from all crop types within the population, hence the larger variation in heading and flowering for this cluster.

Comparison of the clustering of accessions between the two population structures demonstrated the more stringent SNP criteria gave rise to a population structure in which individuals were grouped with other accessions that would be expected to be genetically similar based on knowledge of crop type and flowering phenotype. Consequently, this population structure was applied in subsequent GWAS analyses.

To gauge the extent of linkage disequilibrium we calculated the mean pairwise squared allele-frequency correlation (r^2) for mapped markers. A linkage disequilibrium window of 50 (providing > 3 million pairwise values of r^2) resulted in a mean pairwise r^2 of 0.0979, confirming a low overall level of linkage disequilibrium in *B. oleracea*.

Associative transcriptomics identifies miR172D as a candidate for controlling vernalisation response

SNP associations were compared to the physical positions of orthologues of genes known to be involved in the floral transition in Arabidopsis. A total of 43 flowering time related traits (Additional File 2) were analysed using this pipeline, including DTB and DTF for each treatment. A total of 111 significant SNPs were identified, $P < 0.05$, six of which demonstrated clear association peaks and were investigated further (Table 1).

We first sought to identify genetic associations with the trait data for the non-vernalised experiment. Whilst no significant association peaks were identified for DTB, a single marker association at Bo8g089990.1:453:T was identified (P = 2.29E-06) for DTF under non-vernalising conditions. This marker was within a region demonstrating good synteny to Arabidopsis, despite there being a number of unannotated gene models present. Conservation between Arabidopsis and *B. oleracea* suggests that this region contains an orthologue of microRNA172D, AT3G55512, which has been linked to the floral transition in *A. thaliana* [26,27] (Fig. 3A). Furthermore, the difference in DTB between 10WPG6WV5 ºCV and 10WPG12WV15 ºCV, identified a significant association on C07 at Bo7g104810.1:204:T (FDR, $P < 0.05$). This association was in the vicinity of a second orthologue of miR172D (Fig. 3C).

We then analysed the association with traits relating to the timing of vernalisation. No significant associations were identified for traits after 6WPG12WV5 ºCV. However, a strong association was identified on C07 at the marker Bo7g026810.1:124:G, for DTF for 6WPG12WV10 ºCV. Synteny with Arabidopsis suggests that an orthologue of *FRI INTERACTING PROTEIN 1,* (*FIP1*), AT2G06005.1 (Fig. 3D) is present within this region. Within Arabidopsis it has been demonstrated that *FIP1* interacts with *FRIGIDA* (*FRI*) [28] which is a major source of natural variation in flowering time in Arabidopsis and has been shown to be important in determining vernalisation requirement. Additionally, significant associations (FDR, $P < 0.05$), were found for DTB for 6WPG12WV10 ºCV. An association was identified at Bo9g179000.1:2589:G, which is in the vicinity of an orthologue of *Early Flowering*

6 (*ELF6*), AT5G04240.1 (Fig. 3B), a nuclear targeted protein able to affect flowering time irrespective of *FLC.*

The differences in flowering phenotype between the SNP variants for the four strongest associations were analysed (Fig. 4). There were significant differences in the traits associated with miR172D (DTF with no vernalisation and the difference in DTB for plants grown under 5 ºCV and 15 ºCV) for different alleles (Fig. 4A and B). For Bo7g104810.1:204:T (difference in DTB after exposure to 5 ºCV and 15 ºCV), five individuals, four broccoli and one cauliflower, contained the A variant. The alternate variant, a T allele, and was present in 50 individuals. Conversely, Bo8g089990.1:453:T (DTF with no vernalisation) had 11 individuals with a C allele at this locus, whilst 51 had a T allele. Interestingly, individuals with the C allele were present in every crop type.

Associative transcriptomics identifies Bo*FLC.C2* as a candidate gene involved in vernalisation requirement in *B. oleracea*

An advantage of performing associative transcriptomics as opposed to GWAS, is the additional ability to identify associations between gene expression and the trait of interest. GWAS analysis identified an association of the difference between DTB and DTF with a 10WPG6WV5 ºCV with a candidate marker in the well characterized flowering time gene, *BoFLC.C2* (Table 1). Using gene expression marker (GEM) analysis, *BoFLC.C2* expression was also identified as being significantly associated with both the DTB and DTF under non-vernalising conditions (Fig. 5). *BoFLC.C2* exhibited both low and high expression within the population. As expected, all five rapid cycling accessions demonstrated no *BoFLC.C2* expression. Recently, a Brassica consortium developed targeted sequence capture for a set of relevant genes, including *FLC*. DNA from four of the five rapid cycling accessions had been enriched with that capture library and sequenced. Lacking a reference sequence for *B.*

oleracea that contains *BoFLC.C2*, we used *B. napus* (cv. Darmor) [29] as a reference to map the captured sequence data from the four rapid cycling accessions to. Comparison of *B. oleracea* transcript data [30] to this Darmor genome reference revealed a 99.54 % identity in coding sequence, allowing Darmor to be used as a surrogate reference. Indeed, we found that *BoFLC.C2* was absent from all four rapid cycling accessions, GT050381, GT080767, GT100067 and GT110222, revealed by a lack of read mapping (Additional File 10). *BoFLC.C2* is known to be involved in vernalisation response [30] and rapid cycling varieties do not require a period of vernalisation in order to transition to the floral state. As a control, we investigated mapping for 49 non-rapid cycling accessions where we expect *BoFLC.C2* to be present. For all 49 we found the expected read mapping evidence, confirming that use of the polyploid *B. napus* reference is appropriate (Additional File 10). The control of flowering is a complex, multigenic trait, therefore we would not expect a single locus to explain all variation across the entire dataset. Indeed, only a weak positive correlation (DTB $R^2 = 0.024$, DTF $R^2 = 0.036$) between flowering phenotype and *BoFLC.C2* expression was identified. A strong positive correlation (DTB $R^2 = 0.871$, DTF $R^2 = 0.891$) was found for the phenotypic extremes (rapid cycling lines with no expression and the late flowering lines with high levels of *BoFLC.C2*), Fig. 6, confirming a role for *BoFLC.C2*.

Discussion

Determining which genes underly phenotypic traits is a key step for crop improvement. A powerful approach for identifying candidates is associative transcriptomics, which has been implemented for several crops. However, for the important vegetable crop *B. oleracea,* no such pipeline has been published to date. Here we present a validated associative transcriptomics pipeline for *B. oleracea* and use it to identify gene candidates for vernalisation.

To reduce the risk of false positives, we developed stringent criteria to identify unlinked markers for the determination of the population structure. The population structure was validated using crop type and phenotypic information on heading and flowering, this example was chosen as producing synchronous *B. oleracea* vegetables is a key goal for growers and breeders. Quantifying vernalisation responses for different varieties is an important step towards this goal, providing a foundation for targeted breeding.

Phenotyping for both DTB and DTF under different environmental conditions revealed a varied response within the population and identified some general trends. Altering the timing of vernalisation demonstrated that a shorter growth period prior to the exposure to cold extended the time taken to reach DTB and DTF. This could be attributed to the presence of a juvenile phase in many of the lines, which has been widely documented in *B. oleracea* [14,31,32]. A juvenile plant is described as being unable to respond to floral inductive cues. The fact that many lines were able to flower much faster following longer pre-vernalisation growth, suggests they had reached the adult vegetative phase and were receptive to cold as a floral inductive cue. Further experimental work would be needed to test this hypothesis.

Increasing vernalisation length and reducing vernalisation temperature resulted, on average, in faster and more synchronous heading and flowering. This was a predicted outcome, as current knowledge suggests that increased vernalisation duration and cooler vernalisation temperatures would saturate the vernalisation requirement of a larger proportion of accessions.

Using our validated population structure with associative mapping, we identified candidates orthologous to known Arabidopsis floral regulators, including miR172D. In Arabidopsis, the miR172 family post-transcriptionally supress a number of *APETALA1*-like genes, including *TARGET OF EAT1, 2* and *3*, which in turn aids the promotion of floral induction [27,33–35]. Furthermore, the SNP variant data for both associations implicating miR172D, exhibit

289 significant phenotypic differences. Two orthologues of Arabidopsis *miR172D* have been
290 identified in *B. oleracea* [36] but their functional roles have yet to be determined.

291 GWAS analysis identified a significant association with *BoFLC.C2* and the difference in DTB
292 and DTF following a ten-week pre-growth period, with six weeks of vernalisation at 5 ºC.
293 *BoFLC.C2* is a well characterized flowering time gene [30] and the ability of the GWAS pipeline
294 to identify a known candidate gives confidence in the method. Furthermore, GEM analysis
295 identified *BoFLC.C2* expression as being significantly associated with both DTB and DTF
296 under non-vernalising conditions, which can be attributed to the extreme phenotypes within
297 the population (Fig. 6). No *BoFLC.C2* expression was detected in five lines. A loss-of-function
298 mutation at *BoFLC.C2* in cauliflower has been associated with an early flowering phenotype
299 [37], indicating that *BoFLC.C2* has an equivalent role in cauliflower to *FLC* in Arabidopsis.
300 Four of the five lines for which *BoFLC.C2* expression could not be detected did not have the
301 *BoFLC.C2* paralogue according to the bait capture sequencing data. These four lines were all
302 kales and demonstrated an early flowering phenotype, suggesting that *BoFLC.C2* has a
303 similar role to *AtFLC* in kales, and potentially across *B. oleracea*. Although DTB and DTF were
304 highly correlated with *BoFLC.C2* expression under non-vernalising conditions for the
305 phenotypic extremes, for the whole population the correlation was low. This is to be expected
306 as *BoFLC.C2* is just one of many genes that we expect to be involved in the floral transition
307 within *B. oleracea* and therefore is unlikely to account for all the observed variation.

308 The expression data used for the GEM analysis was generated from leaf tissue at one
309 timepoint. As a consequence, any genes which are not expressed in the leaf at this time will
310 not be identified in this analysis. Use of transcriptome data from other tissues in addition to
311 the leaf data could identify a greater number of associations.

312

313 ## Conclusion

Identifying genes underlying phenotypic traits in *B. oleracea* is an important step for the improvement of brassica vegetables. Here, we generate and validate a novel pipeline for associative transcriptomics analysis in *B. oleracea* and show that this pipeline is effective in identifying genetic regulators of complex traits, such as flowering time*,* demonstrating this approach can be utilised for other traits of agronomic importance, such as germination, quality traits and disease resistance. GWAS analysis identified miR172D as a candidate for vernalisation response, whilst GWAS and GEM analysis identified a significant marker at *BoFLC.C2*, an important gene in the vernalisation pathway of *B. oleracea*. Our results provide insight into the genetic control of flowering in *B. oleracea,* and candidates which could provide a foundation for future breeding strategies.

Methods

Plant Materials and Growth Conditions

A subset of 69 lines fixed as doubled haploids (DH) or at S4 and above were chosen from the *Brassica oleracea* Diversity Fixed Foundation Set [14] (Additional File 1) comprising accessions from seven different *B. oleracea* crop types; cabbage, cauliflower, calabrese, broccoli, kohl rabi, kale and Brussels sprout. Plants were grown in cereals mix (40 % Medium Grade Peat, 40 % Sterilised Soil, 20 % Horticultural Grit, 1.3 kg/m³ PG Mix 14-16-18 + Te Base Fertiliser, 1 kg/m³ Osmocote Mini 16-8-11 2 mg + Te 0.02 % B, Wetting Agent, 3 kg/m³ Maglime, 300 g/m³ Exemptor) and given a pre-growth period of either six or ten weeks in a glasshouse under natural light supplemented with LED lighting (16h daylength 21/18 °C day/night). At the end of the pre-growth period, three plants of each line for each treatments were transferred to Conviron controlled environment rooms for six or twelve weeks

vernalisation at 5, 10 or 15 ºC (16 h daylength LED, 60 % humidity). Following vernalisation, plants were re-potted into 2 L pots and placed into a polytunnel under natural light using a randomised block design. All plants came out of vernalisation and into the polytunnel on the same day due to staggered sowing to control for post-vernalisation environmental conditions. Three replicates of each line were grown without vernalisation as a non-vernalised control group. The plants were scored at buds visible (DTB) and upon opening of first flower (DTF) [38]. A summary of pre-growth and vernalisation conditions and traits analysed is given in Additional File 2.

SNP Calling

The growth conditions, sampling of plant material, RNA extraction and transcriptome sequencing was carried out as described by He et al. [39]. The RNA-seq data from each accession were mapped on to CDS models from the *Brassica oleracea* pangenome [40] as reference sequences, using Maq v0.7.1 [41]. SNPs were called by the meta-analysis of alignments as described in Bancroft et al. [42]. SNP positions were excluded if they had a read depth < 10, a base call quality < Q20, missing data > 0.25, and > 3 alleles. This resulted in a SNP file containing 110,555 SNPS, and 65017 unigene sequences with associated RPKM values.

Population Structure and GWAS analyses

Population structure was generated using both relaxed (all markers with a minor allele frequency (MAF) > 0.05) and stringent criteria using STRUCTURE [43] (burn-in10000, MCMC 10000, 10 iterations). For the stringent criteria, SNPs were required to be biallelic, with a minor allele frequency (MAF) > 0.05 and a minimum distance of 500-bp between markers.

362 STRUCTURE HARVESTER [44] was used to determine the optimal *K* value. The Q matrix
363 used in GWAS analysis was calculated using CLUMPP [45].

364 TASSEL [46] version 5.0 was used to select the most appropriate model for each trait based
365 on QQ plots. Generalised linear models (GLM), with correction for population structure using
366 the Q matrix or PCA (5 PCs) were used to look for associations. For GWAS analysis only SNP
367 markers with an allele frequency > 0.05 were used. To gauge the extent of linkage
368 disequilibrium, the mean pairwise r^2 was calculated using the SlidingWindow function within
369 TASSEL, with a linkage disequilibrium window of 50. TASSEL was used to construct
370 phylogenetic trees, using the Neighbour Joining method and all SNPs with MAF > 0.05. Trees
371 were graphed in R using the package ggtree [47].

372 Gene expression marker (GEM) associations were calculated by an in-house script in R
373 Version 3.6.3 using a fixed effect linear model with RPKM values, excluding markers with an
374 average expression below 0.5 RPKM. Linear regression was performed using RPKM as a
375 predictor value to predict a quantitative outcome of the trait value. Both SNP and GEM outputs
376 were plotted as Manhattan Plots created using an in-house R script. All scripts are available
377 at https://github.com/JIC-CSB/Boleracea-AssociativeTranscriptomics. Statistical significance
378 for both GWAS and GEM association was determined by the false discovery rate (FDR) [48]
379 calculated using the QValue package [49] in R.

380

381 **DNA Extraction**

382 Genomic DNA of accessions used in bait capture sequencing was prepared from young leaf
383 tissue of plants grown in a glasshouse (16h LED supplementary light, 21/18 °C day/night).
384 Light was excluded for 48 h prior to harvesting. Nuclei were extracted from ~3 g of tissue prior
385 to CTAB based DNA extraction. Extracts were treated with RNase T1, RNaseA and

Proteinase K to remove RNA and protein contamination, respectively. DNA was resuspended in 50 μl dH_2O and checked for quality. DNA was quantified by and stored at -20 °C.

Targeted Sequence Enrichment analysis

A bait library for targeted sequence enrichment for a specific subset of genes was developed and synthesized with Arbor Biosciences (https://arborbiosci.com/). Samples were 4 plexed and run on the NovaSeq S4, PE150, 1Gbp/library. Reads from individual accessions were mapped to the reference sequence of *B. napus* cv. Darmor-*bzh* [29] using BWA [50] version 0.7.17-r1188 using aln/sampe and standard parameters. Mapped reads were sorted and indexed using SAMTOOLS [51] version 1.10 sort and index, and subsequently visualized with Integrative Genomics Viewer (IGV) [52].

References

1. Wichmann MC, Alexander MJ, Hails RS, Bullock JM. Historical distribution and regional dynamics of two Brassica species. Ecography (Cop). John Wiley & Sons, Ltd; 2008;31:673–84.

2. Chouard P. Vernalization and its Relations to Dormancy. Annu Rev Plant Physiol. Annual Reviews 4139 El Camino Way, P.O. Box 10139, Palo Alto, CA 94303-0139, USA; 1960;11:191–238.

3. Korte A, Farlow A. The advantages and limitations of trait analysis with GWAS: a review. 2013.

4. Harper AL, Trick M, Higgins J, Fraser F, Clissold L, Wells R, et al. Associative transcriptomics of traits in the polyploid crop species *Brassica napus*. Nat Biotechnol. Nature

410 Publishing Group; 2012;30:798–802.

411 5. Huang X, Zhao Y, Wei X, Li C, Wang A, Zhao Q, et al. Genome-wide association study of
412 flowering time and grain yield traits in a worldwide collection of rice germplasm. Nat Genet.
413 Nature Publishing Group; 2012;44:32–9.

414 6. Raman H, Raman R, Qiu Y, Yadav AS, Sureshkumar S, Borg L, et al. GWAS hints at
415 pleiotropic roles for *FLOWERING LOCUS T* in flowering time and yield-related traits in
416 canola. BMC Genomics. 2019;20.

417 7. Romero Navarro JA, Willcox M, Burgueño J, Romay C, Swarts K, Trachsel S, et al. A
418 study of allelic diversity underlying flowering-time adaptation in maize landraces. Nat Genet.
419 2017;49:476–80.

420 8. Miller CN, Harper AL, Trick M, Werner P, Waldron K, Bancroft I. Elucidation of the genetic
421 basis of variation for stem strength characteristics in bread wheat by Associative
422 Transcriptomics. BMC Genomics. BioMed Central; 2016;17:500.

423 9. Zhao K, Tung CW, Eizenga GC, Wright MH, Ali ML, Price AH, et al. Genome-wide
424 association mapping reveals a rich genetic architecture of complex traits in *Oryza sativa*. Nat
425 Commun. Nature Publishing Group; 2011;2:467.

426 10. Cockram J, White J, Zuluaga DL, Smith D, Comadran J, MacAulay M, et al. Genome-
427 wide association mapping to candidate polymorphism resolution in the unsequenced barley
428 genome. Proc Natl Acad Sci U S A. National Academy of Sciences; 2010;107:21611–6.

429 11. Yu J, Buckler ES. Genetic association mapping and genome organization of maize. Curr
430 Opin Biotechnol. Elsevier Current Trends; 2006;17:155–60.

431 12. Flint-Garcia SA, Thornsberry JM, Buckler ES. Structure of Linkage Disequilibrium in
432 Plants. Annu Rev Plant Biol. 2003;54:357–74.

433 13. Evanno G, Regnaut S, Goudet J. Detecting the number of clusters of individuals using

434 the software structure: a simulation study. Mol Ecol. John Wiley & Sons, Ltd; 2005;14:2611–
435 20.

436 14. Walley PG, Teakle GR, Moore JD, Allender CJ, Pink DA, Buchanan-Wollaston V, et al.
437 Developing genetic resources for pre-breeding in *Brassica oleracea* L.: An overview of the
438 UK perspective. J. Plant Biotechnol. 2012. p. 62–8.

439 15. Putterill J, Laurie R, Macknight R. It's time to flower: the genetic control of flowering time.
440 BioEssays. Wiley Subscription Services, Inc., A Wiley Company; 2004;26:363–73.

441 16. Rosen A, Hasan Y, Briggs W, Uptmoor R. Genome-Based Prediction of Time to Curd
442 Induction in Cauliflower. Front Plant Sci. Frontiers; 2018;9:78.

443 17. Xu L, Hu K, Zhang Z, Guan C, Chen S, Hua W, et al. Genome-wide association study
444 reveals the genetic architecture of flowering time in rapeseed (*Brassica napus* L.). DNA Res.
445 Oxford Academic; 2015;23:43–52.

446 18. Chen J, Zheng H, Bei J-X, Sun L, Jia W, Li T, et al. Genetic Structure of the Han
447 Chinese Population Revealed by Genome-wide SNP Variation. Am J Hum Genet. Cell
448 Press; 2009;85:775–85.

449 19. Breria CM, Hsieh CH, Yen J-Y, Nair R, Lin C-Y, Huang S-M, et al. Population Structure
450 of the World Vegetable Center Mungbean Mini Core Collection and Genome-Wide
451 Association Mapping of Loci Associated with Variation of Seed Coat Luster. Trop Plant Biol.
452 Springer; 2020;13:1–12.

453 20. Lu G, Harper AL, Trick M, Morgan C, Fraser F, O'Neill C, et al. Associative
454 transcriptomics study dissects the genetic architecture of seed glucosinolate content in
455 brassica napus. DNA Res. Narnia; 2014;21:613–25.

456 21. Prom LK, Ahn · Ezekiel, Thomas Isakeit ·, Magill · Clint. GWAS analysis of sorghum
457 association panel lines identifies SNPs associated with disease response to Texas isolates

458 of *Colletotrichum sublineola*. Theor Appl Genet. 2019;132:1389–96.

459 22. Cullingham CI, Miller JM, Peery RM, Dupuis JR, Malenfant RM, Gorrell JC, et al.
460 Confidently identifying the correct K value using the ΔK method: When does K = 2? Mol
461 Ecol. Blackwell Publishing Ltd; 2020;29:862–9.

462 23. Janes JK, Miller JM, Dupuis JR, Malenfant RM, Gorrell JC, Cullingham CI, et al. The K =
463 2 conundrum. Mol Ecol. Blackwell Publishing Ltd; 2017;26:3594–602.

464 24. Labana KS, Gupta ML. Importance and Origin. Springer, Berlin, Heidelberg; 1993. p. 1–
465 7.

466 25. Maggioni L, von Bothmer R, Poulsen G, Branca F. Origin and domestication of cole
467 crops (*Brassica oleracea* L.): Linguistic and literary considerations. Econ Bot. Springer;
468 2010;64:109–23.

469 26. Poethig RS. Small RNAs and developmental timing in plants. Curr Opin Genet Dev.
470 Elsevier Current Trends; 2009;19:374–8.

471 27. Aukerman MJ, Sakai H. The Plant Cell Regulation of Flowering Time and Floral Organ
472 Identity by a MicroRNA and Its *APETALA2-Like* Target Genes. Plant Cell. 2003;15:2730–41.

473 28. Geraldo N, Bäurle I, Kidou SI, Hu X, Dean C. FRIGIDA delays flowering in Arabidopsis
474 via a cotranscriptional mechanism involving direct interaction with the nuclear cap-binding
475 complex. Plant Physiol. American Society of Plant Biologists; 2009;150:1611–8.

476 29. Chalhoub B, Denoeud F, Liu S, Parkin IAP, Tang H, Wang X, et al. Erratum: Early
477 allopolyploid evolution in the post-Neolithic *Brassica napus* oilseed genome (Science (2014)
478 345:6199 (950-953)). Science (80-.). 2014. p. 6199.

479 30. Irwin JA, Soumpourou E, Lister C, Ligthart JD, Kennedy S, Dean C. Nucleotide
480 polymorphism affecting *FLC* expression underpins heading date variation in horticultural
481 brassicas. Plant J. 2016;87:597–605.

482 31. Wurr DCE, Fellows JR, Sutherland RA, Elphinstone ED. A model of cauliflower curd
483 growth to predict when curds reach a specified size. J Hortic Sci. Taylor & Francis;
484 2016;65:555–64.

485 32. Hand DJ, Atherton JG. Curd initiation in the cauliflower: I. Juvenility. J Exp Bot. Narnia;
486 1987;38:2050–8.

487 33. Teotia S, Tang G. To bloom or not to bloom: Role of micrornas in plant flowering. Mol.
488 Plant. 2015. p. 359–77.

489 34. Jung J-H, Seo Y-H, Seo PJ, Reyes JL, Yun J, Chua N-H, et al. The GIGANTEA-
490 Regulated MicroRNA172 Mediates Photoperiodic Flowering Independent of *CONSTAN*S in
491 Arabidopsis W OA.

492 35. Wu G, Park MY, Conway SR, Wang J-W, Weigel D, Poethig RS. The Sequential Action
493 of miR156 and miR172 Regulates Developmental Timing in Arabidopsis. Cell. Cell Press;
494 2009;138:750–9.

495 36. Shivaraj S, Dhakate P, Mayee P, Negi M, Singh A. Natural genetic variation in MIR172
496 isolated from Brassica species. Biol Plant. 2014;58:627–40.

497 37. Ridge S, Brown PH, Hecht V, Driessen RG, Weller JL. The role of *BoFLC2* in cauliflower
498 (*Brassica oleracea var. botrytis* L.) reproductive development. J Exp Bot. Oxford University
499 Press; 2015;66:125–35.

500 38. Meier U. Growth stages of mono-and dicotyledonous plants BBCH Monograph Federal
501 Biological Research Centre for Agriculture and Forestry. 2001.

502 39. He Z, Wang L, Harper AL, Havlickova L, Pradhan AK, Parkin IAP, et al. Extensive
503 homoeologous genome exchanges in allopolyploid crops revealed by mRNAseq-based
504 visualization. Plant Biotechnol J. 2017;

505 40. Golicz AA, Bayer PE, Barker GC, Edger PP, Kim HR, Martinez PA, et al. The

506 pangenome of an agronomically important crop plant *Brassica oleracea*. Nat Commun.
507 Nature Publishing Group; 2016;7:13390.

508 41. Li, H., Ruan J, Durbin R. Maq: Mapping and assembly with qualities. Version 0.6, 3.
509 2008.

510 42. Bancroft I, Morgan C, Fraser F, Higgins J, Wells R, Clissold L, et al. Dissecting the
511 genome of the polyploid crop oilseed rape by transcriptome sequencing. Nat Biotechnol.
512 Nature Publishing Group; 2011;29:762–6.

513 43. Pritchard JK, Stephens M, Donnelly P. Inference of population structure using multilocus
514 genotype data. Genetics. 2000;155:945–59.

515 44. Earl DA, vonHoldt BM. STRUCTURE HARVESTER: a website and program for
516 visualizing STRUCTURE output and implementing the Evanno method. Conserv Genet
517 Resour. Springer; 2012;4:359–61.

518 45. Jakobsson M, Rosenberg NA. Genetics and population analysis CLUMPP: a cluster
519 matching and permutation program for dealing with label switching and multimodality in
520 analysis of population structure. 2007;23:1801–6.

521 46. Bradbury PJ, Zhang Z, Kroon DE, Casstevens TM, Ramdoss Y, Buckler ES. TASSEL:
522 software for association mapping of complex traits in diverse samples. Bioinformatics.
523 Oxford Academic; 2007;23:2633–5.

524 47. Yu G, Smith DK, Zhu H, Guan Y, Lam TTY. ggtree: an r package for visualization and
525 annotation of phylogenetic trees with their covariates and other associated data. Methods
526 Ecol Evol. British Ecological Society; 2017;8:28–36.

527 48. Benjamini Y, Yekutieli D, Edwards D, Popper Shaffer J. False Discovery Rate-Adjusted
528 Multiple Confidence Intervals for Selected Para. J. Am. Stat. Assoc. 2005.

529 49. Storey J, Bass A, Dabney A, Robinson D. Qvalue [Internet]. qvalue Q-value Estim. false

530 Discov. rate Control. R Packag. version 2.18.0. 2019 [cited 2020 Mar 20]. Available from:
531 http://github.com/jdstorey/qvalue

532 50. Li H, Durbin R. Fast and accurate short read alignment with Burrows-Wheeler transform.
533 Bioinformatics. Oxford University Press; 2009;25:1754–60.

534 51. Li H, Handsaker B, Wysoker A, Fennell T, Ruan J, Homer N, et al. The Sequence
535 Alignment/Map format and SAMtools. Bioinformatics. Oxford Academic; 2009;25:2078–9.

536 52. Robinson JT, Thorvaldsdóttir H, Winckler W, Guttman M, Lander ES, Getz G, et al.
537 Integrative genomics viewer. Nat Biotechnol. NIH Public Access; 2011;29:24–6.

538 53. Woodhouse S. JIC-CSB/Boleracea-AssociativeTranscriptomics: Brassica oleracea
539 Associative Transcriptomics [Internet]. 2021 [cited 2021 Feb 12]. Available from:
540 https://zenodo.org/record/4529809#.YCZ9ry2l1ao

541 54. Steuernagel B, Woodhouse S, He Z, Hepworth J, Tidy A, Siles-Suarez L, et al. BRAVO
542 target sequence capture V3 [Internet]. 2021 [cited 2021 Feb 12]. Available from:
543 https://zenodo.org/record/4473283#.YCZ91S2l1ap

544

545 Figure Legends

546

547 **Figure 1**: Flowering time traits exhibit a varied response to different environmental
548 conditions within the population. Examples of opposing phenotypic response to different
549 vernalisation temperatures can be observed in A) Brussels Sprout, Cavolo Di Bruxelles
550 Precoce (GT120168) and B) Broccoli, Mar DH (GT110244). Variation across the population
551 for C) DTB post vernalisation per treatment, per line. D) DTF post vernalisation per
552 treatment, per line. Day 0 represents the end of vernalisation, negative values represent
553 heading or flowering during the pre-growth or vernalisation.

554

555 **Figure 2**: The choice of SNP pruning rules can significantly change the inferred population
556 structure. Density plots representing A) DTB, C) DTF for the accessions within the five
557 subpopulation clusters. Density plots representing B) DTB, D) DTF for the accessions within
558 the four subpopulation clusters. E) Population structure generated from SNPs with MAF >
559 0.05 F) Population structure generated from more stringent SNP pruning (Biallelic only, MAF
560 > 0.05, > 500-bp apart, one per gene).

561

562 **Figure 3**: The developed pipeline identifies associations with flowering traits. Distribution of
563 mapped markers associating with A) Number of DTF under non-vernalising conditions B)
564 DTB after a six-week pre-growth, twelve weeks vernalisation 10 ºC C) The difference in DTB
565 between six and twelve weeks of vernalisation at 15 ºC, after exposure to a ten-week pre-
566 growth D) The DTF after exposure to six-week pre-growth, twelve weeks vernalisation 10 ºC.
567 Sixty-nine accessions of *B. oleracea* were phenotyped for DTB and DTF and marker
568 associations were calculated using a generalized linear model, implemented in TASSEL to
569 incorporate population structure. Log_{10} (P values) were plotted against the nine *B. oleracea*
570 chromosomes in SNP order. Blue line FDR threshold, P< 0.05, FDR threshold was not met
571 for A) and D).

572

573 **Figure 4:** A significant phenotypic difference was found for individuals exhibiting SNP
574 variants for the associations pointing to miR172D as a candidate. Boxplots represent the
575 trait data, DTB or DTF for each of the significant markers alongside the different alleles
576 present across the population for each marker. The box represents interquartile range,
577 outliers are represented by black dots.

578

Figure 5: GEM analysis identifies *FLC* expression on chromosome C2 as a candidate for flowering traits under non-vernalising conditions. Distribution of gene expression markers associating with A) DTB after exposure to non-vernalising conditions B) DTF after exposure to non-vernalising conditions. Log_{10} (P values) were plotted against the nine *B. oleracea* chromosomes in SNP order. Blue line FDR threshold, $P < 0.05$.

Figure 6: A strong positive correlation can be seen between lines at the phenotypic extremes and their Bo*FLC.C2* expression levels. Colours represent the subpopulation of each line, as determined by population structure analysis.

Table 1: Significant SNP associations with vernalisation response in diverse *B. oleracea* accessions, detected across the genome (FDR < 0.05), including model information.

Declarations

Ethics approval and consent to participate

The plant material within this paper was obtained under material transfer agreement (MTA) from Warwick Germplasm Research Unit (GRU), part of the European Cooperative Program for Plant Genetic Resources (ECPFR). As such, it complies with relevant institutional, national, and international guidelines and legislation. The appropriate permissions and/or licences for collection of plant or seed specimens have been observed by Warwick GRU for their collections and by the authors under MTA for their subsequent use.

Consent for publication

N/A

Availability of data and materials

Sequence data from this article can be found in the SRA data library under accession number PRJNA309368, https://www.ncbi.nlm.nih.gov/bioproject/PRJNA309368. The R scripts used to carry out GEM analysis and to generate the corresponding Manhattan plots for both GEM and GWAS analysis are available on GitHub in the JIC_CSB/Boleracea-AssociativeTranscriptomics repository, DOI 10.5281/zenodo.4529809 [53]. Raw data for targeted sequence capture experiments has been deposited at EBI, under study number PRJEB43076, https://www.ebi.ac.uk/ena/browser/view/PRJEB43076, and the bait library is available at DOI 10.5281/zenodo.4473283 [54].

Competing interests

The authors declare that they have no conflicts of interest.

Funding

SW was supported by the UK Biotechnology and Biological Sciences Research Council (BBSRC) NRPDTP PhD Studentship Programme. JI and RW acknowledge funding from BBSRC Institute Strategic Programme (BB/P013511/1), RM, JI and RW acknowledge support from the BBSRC sLoLa 'Brassica Rapeseed and Vegetable Optimisation' (BB/P003095/1) and IB and ZH acknowledge funding from BBSRC (BB/L002124/1). RM

624 acknowledges support from EU-Horizon2020 ERC Synergy Grant ‘PLAMORF’ (ID: 810131).
625 Additional funding was provided by BBSRC sLoLa ‘Renewable Industrial Products from
626 Rapeseed’ (BB/L002124/1).

627

628 Authors’ contributions

629 JI, RM, RW and SW designed the experiments that were carried out by SW with support
630 from JI and RW. The SNP calling was carried out by ZH under guidance of IB. SW
631 performed the phenotyping of material, all analyses and produced all figures. RW, IB and
632 WH provided genomics and bioinformatics advice. HW provided programming support and
633 guidance. BS designed and constructed the bait library for targeted sequence enrichment
634 and carried out subsequent sequence mapping, which was analysed by SW. SW drafted the
635 manuscript which was planned and refined by SW, RW and all authors contributed to writing
636 the manuscript.

637

638 Acknowledgements

639 We thank Profs Lars Ostergaard and Steve Penfield (JIC) and Drs Andrea Harper and
640 Lenka Havlickova (York) for discussion and critical comments on the manuscript. We thank
641 Dr Alex Calderwood (JIC) for guidance and advice. We also thank University of Warwick
642 Germplasm Resources Unit for use of the *B. oleracea* Diversity Fixed Foundation Set [14].

Figure1

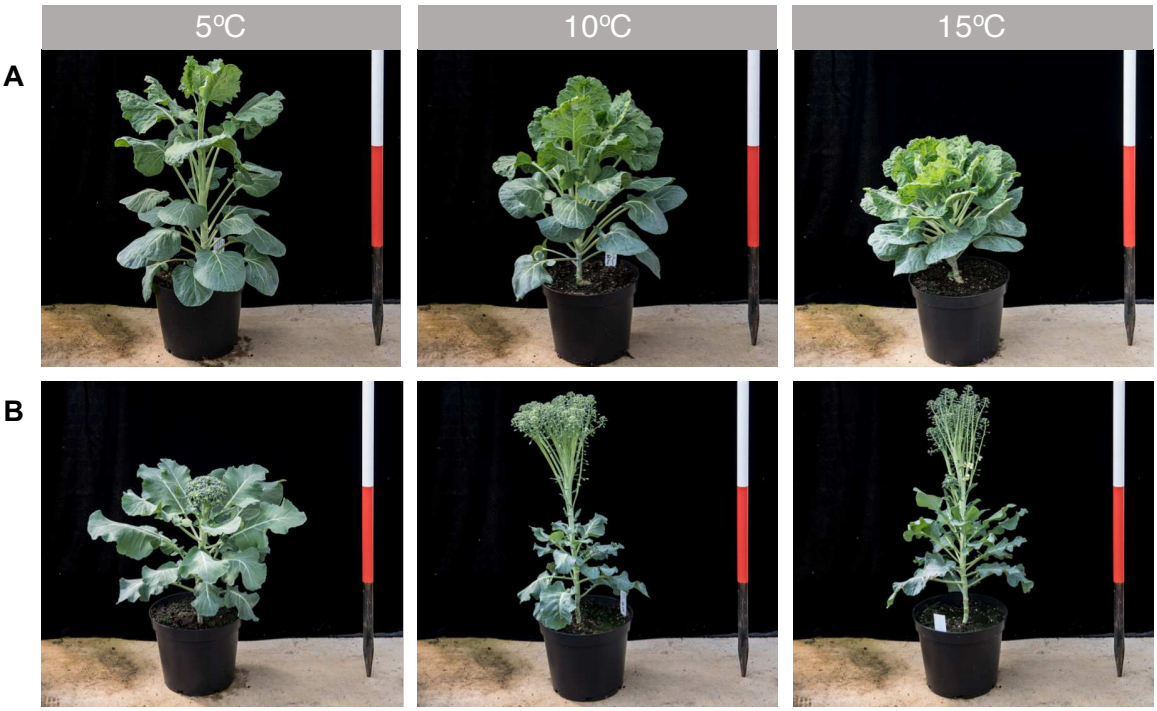
5ºC
10ºC
15ºC
A
B

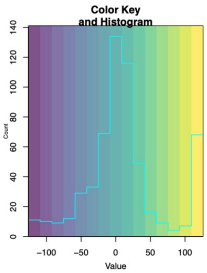
Color Key and Histogram
Count
Value

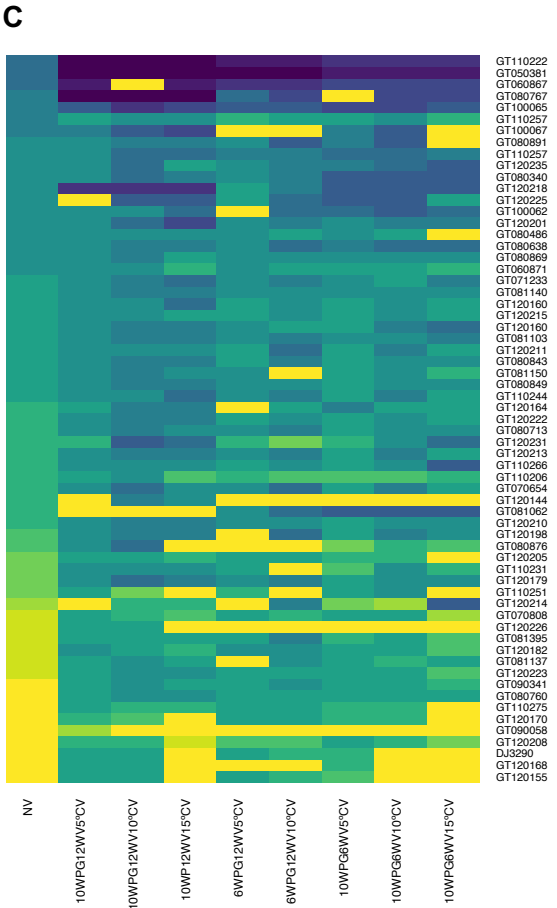
C
GT110222
GT050381
GT060867
GT080767
GT100065
GT110257
GT100067
GT080891
GT110257
GT120235
GT080340
GT120218
GT120225
GT100062
GT120201
GT080486
GT080638
GT080869
GT060871
GT071233
GT081140
GT120160
GT120215
GT120160
GT081103
GT120211
GT080843
GT081150
GT080849
GT110244
GT120164
GT120222
GT080713
GT120231
GT120213
GT110266
GT110206
GT070654
GT120144
GT081062
GT120210
GT120198
GT080876
GT120205
GT110231
GT120179
GT110251
GT120214
GT070808
GT120226
GT081395
GT120182
GT081137
GT120223
GT090341
GT080760
GT110275
GT120170
GT090058
GT120208
DJ3290
GT120168
GT120155
NV
10WPG12WV5ºCV
10WPG12WV10ºCV
10WP12WV15ºCV
6WPG12WV5ºCV
6WPG12WV10ºCV
10WPG6WV5ºCV
10WPG6WV10ºCV
10WPG6WV15ºCV


D
GT050381
GT110221
GT060867
GT080767
GT120215
GT110257
GT100067
GT080891
GT100062
GT080486
GT120235
GT120225
GT060871
GT080341
GT120201
GT100120
GT081103
GT120160
GT120162
GT081140
GT080843
GT080693
GT110244
GT120164
GT080849
GT081150
GT100065
GT120211
GT120222
GT120210
GT120144
GT120198
GT120163
GT120213
GT120192
GT080869
GT120179
GT081062
GT110266
GT080713
GT120231
GT120226
GT081395
GT110206
GT120214
GT080760
GT061882
GT070804
GT080876
GT120182
DJ3290
GK040099
GT090058
GT090341
GT110251
GT110275
GT120155
GT120168
GT120170
GT120205
GT120208
GT120218
GT120223
NV
10WPG12WV5ºCV
10WPG12WV10ºCV
10WP12WV15ºCV
6WPG12WV5ºCV
6WPG12WV10ºCV
10WPG6WV5ºCV
10WPG6WV10ºCV
10WPG6WV15ºCV

Figure2

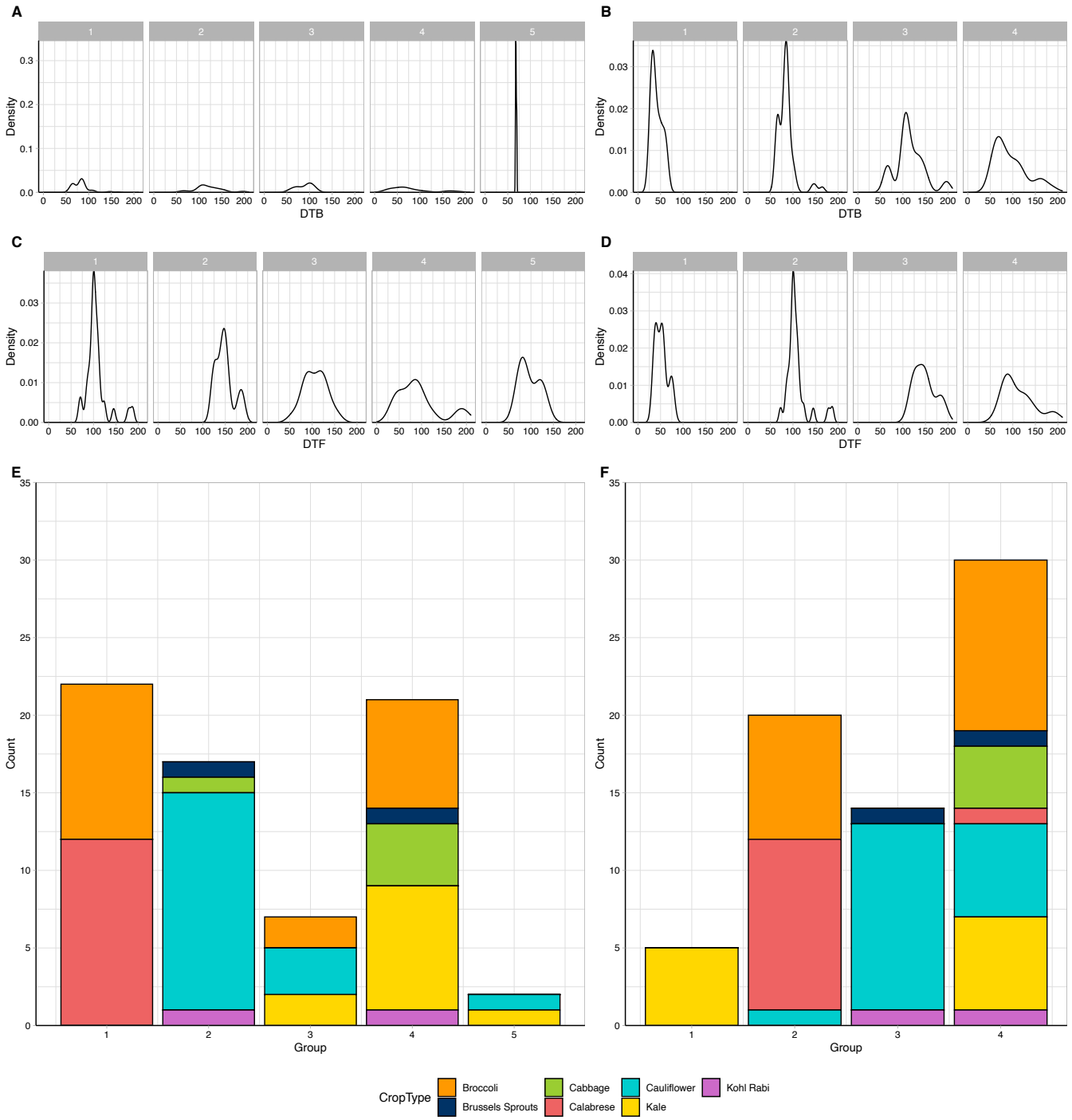
A
B
C
D
E
F
Density
DTB
DTF
Count
Group
CropType
Broccoli
Brussels Sprouts
Cabbage
Calabrese
Cauliflower
Kale
Kohl Rabi

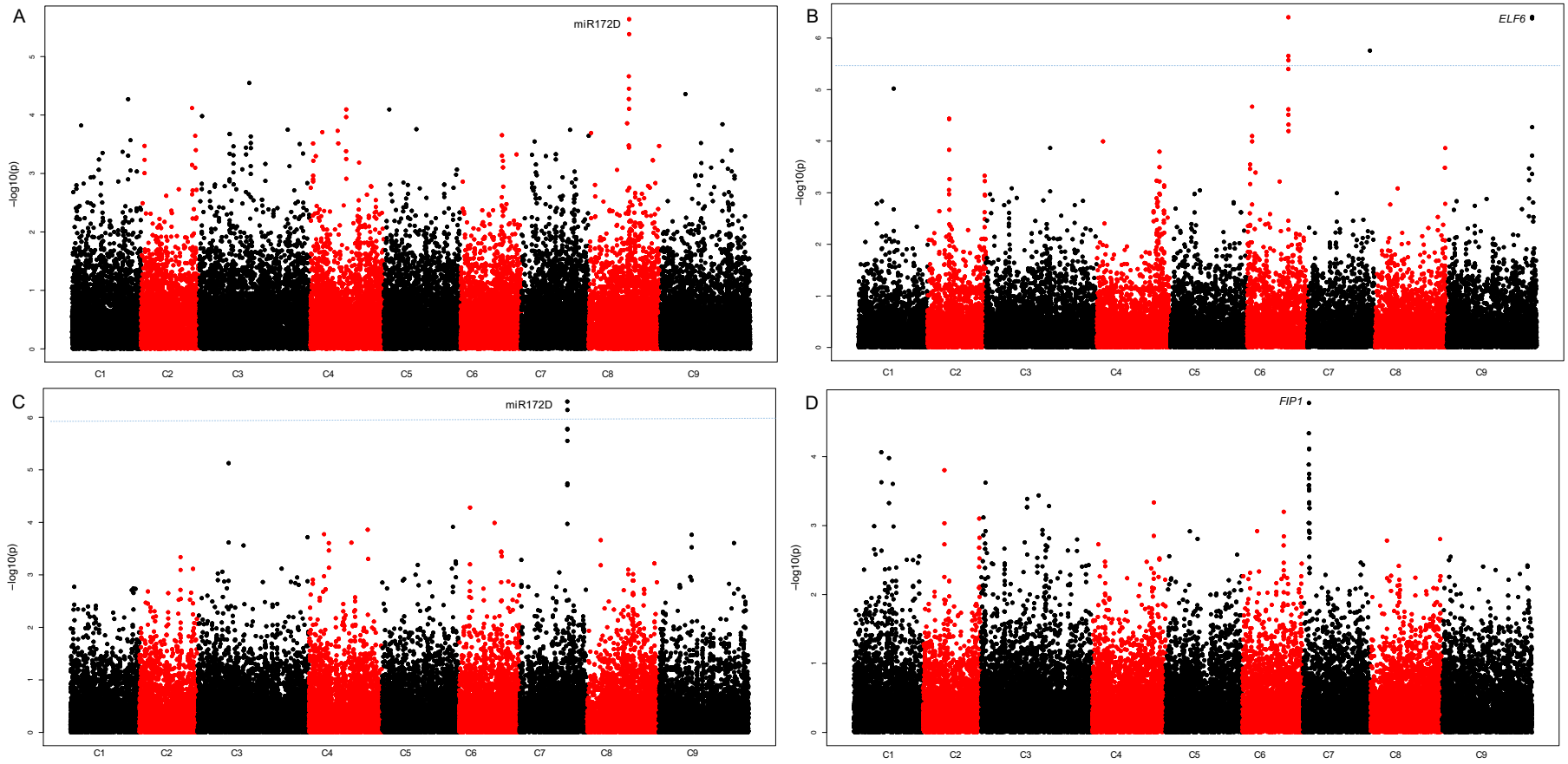
A
miR172D
−log10(p)
C1
C2
C3
C4
C5
C6
C7
C8
C9
B
ELF6
−log10(p)
C1
C2
C3
C4
C5
C6
C7
C8
C9
C
miR172D
−log10(p)
C1
C2
C3
C4
C5
C6
C7
C8
C9
D
FIP1
−log10(p)
C1
C2
C3
C4
C5
C6
C7
C8
C9

Figure3

Figure4

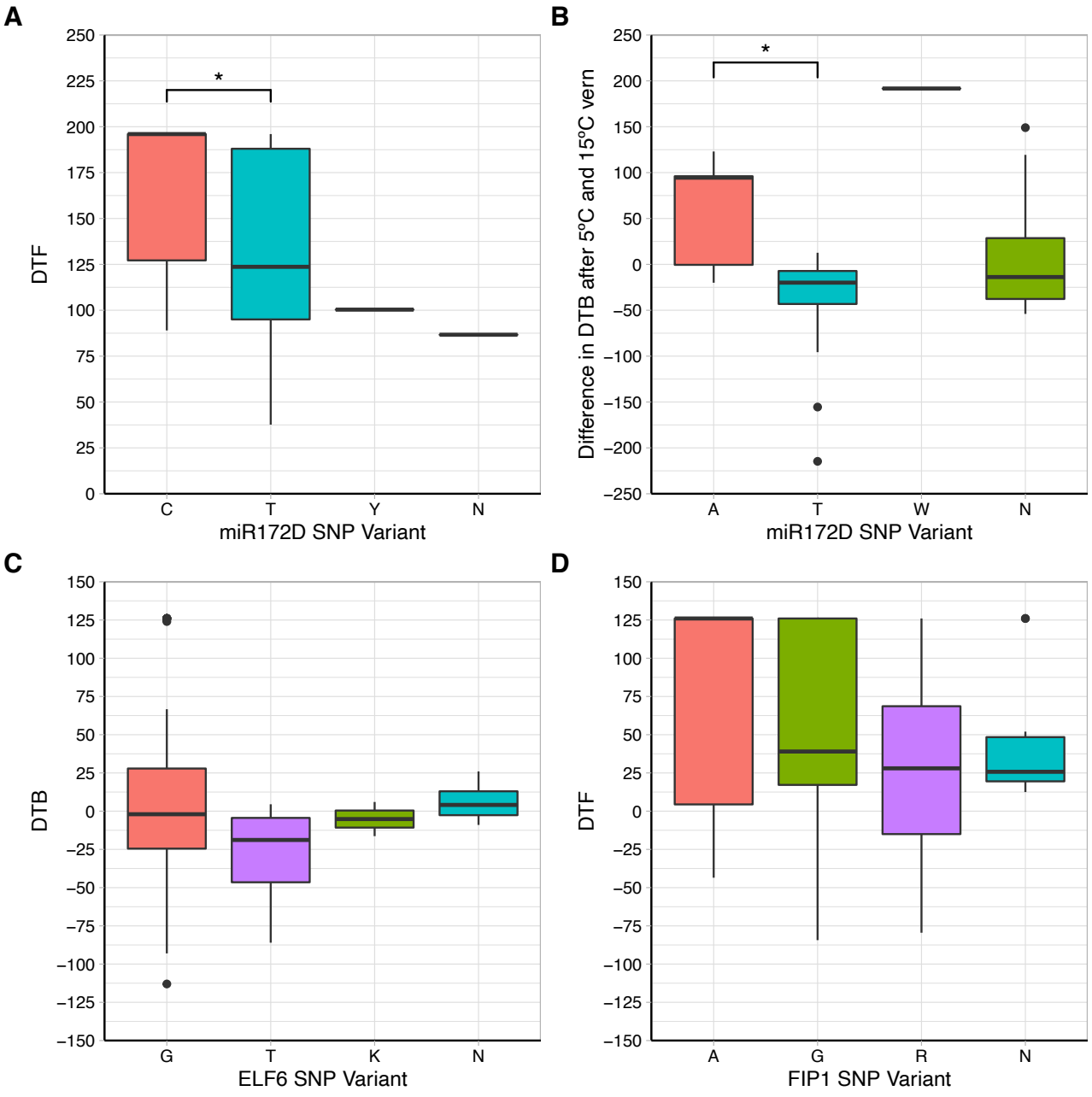
A
DTF
250
225
200
175
150
125
100
75
50
25
0
*
C
T
Y
N
miR172D SNP Variant
B
Difference in DTB after 5°C and 15°C vern
250
200
150
100
50
0
−50
−100
−150
−200
−250
*
A
T
W
N
miR172D SNP Variant
C
DTB
150
125
100
75
50
25
0
−25
−50
−75
−100
−125
−150
G
T
K
N
ELF6 SNP Variant
D
DTF
150
125
100
75
50
25
0
−25
−50
−75
−100
−125
−150
A
G
R
N
FIP1 SNP Variant

Figure5

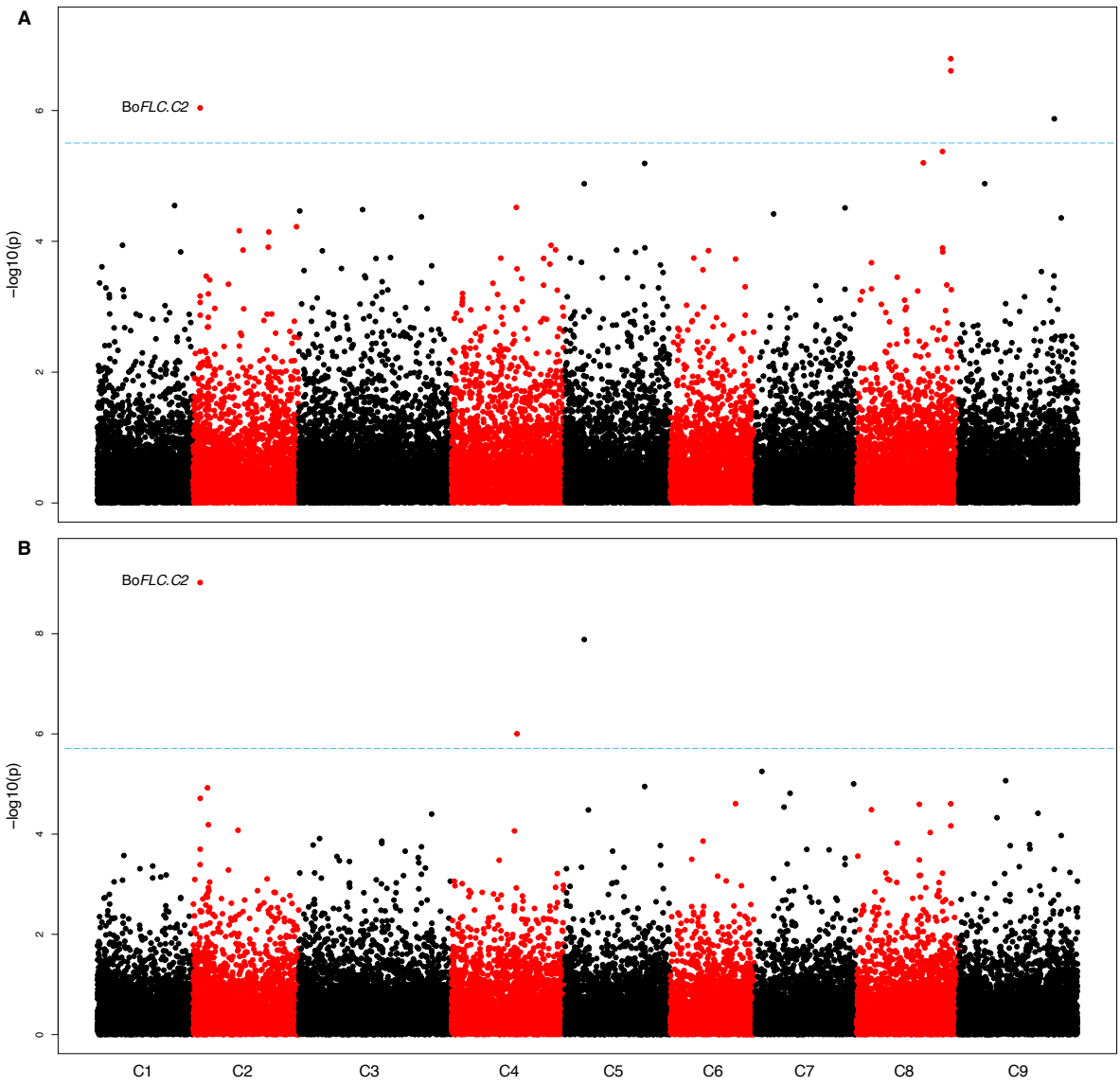
A
BoFLC.C2
−log10(p)
0
2
4
6
B
BoFLC.C2
−log10(p)
0
2
4
6
8
C1
C2
C3
C4
C5
C6
C7
C8
C9

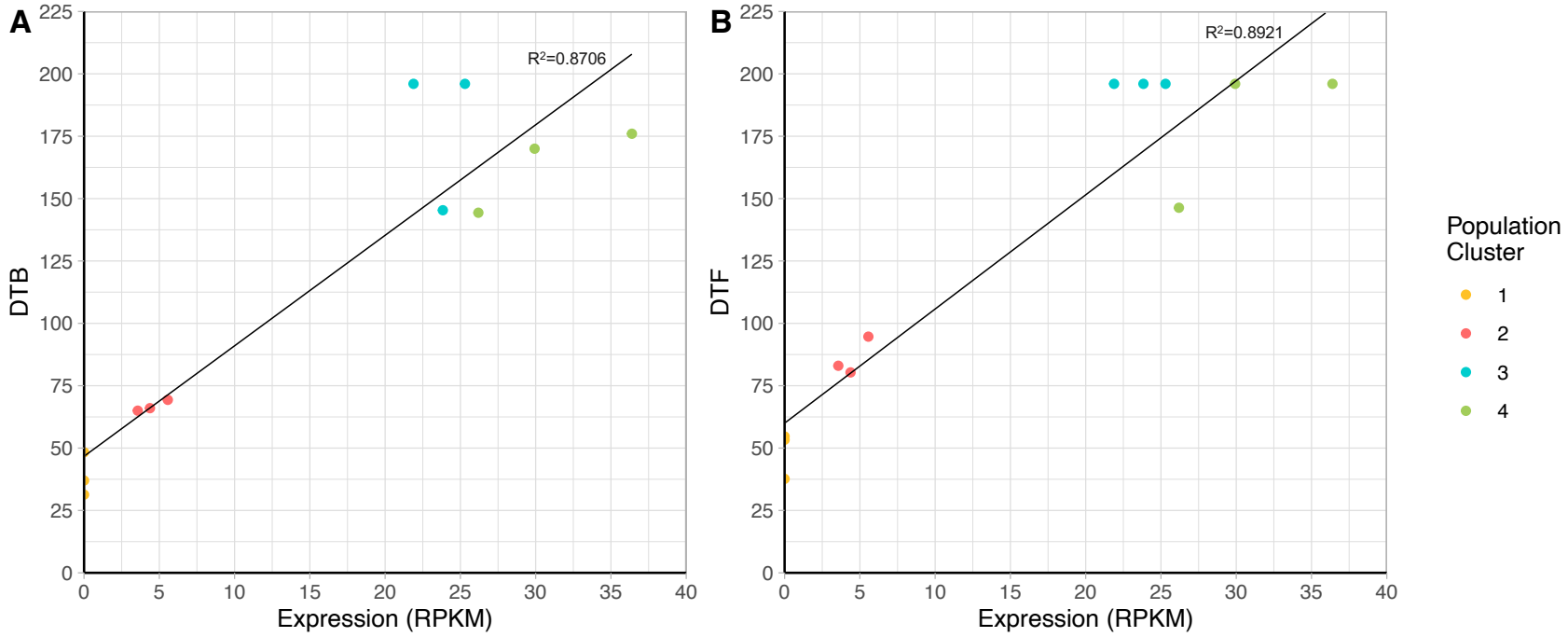
A
B
DTB
DTF
Expression (RPKM)
Expression (RPKM)
R²=0.8706
R²=0.8921
0
25
50
75
100
125
150
175
200
225
0
5
10
15
20
25
30
35
40
Population
Cluster
1
2
3
4

Figure6

Marker Information			Association Information					Model Information	
Marker	**Chromosome**	**Alleles**	**-Log10(p)**	**Marker R^2**	**Traits**	**Arabidopsis ID**	**Orthologue**	**Model**	**Population Structure Correction**
Bo6g103650.1:2010:T	C06	C/T/Y	6.4017787	0.39231	6P 12V 10 ºC DTB	AT1G67140.3	*SWEETIE*	GLM	Q-Matrix
Bo9g179000.1:2589:G	C09	G/T/K	6.4077566	0.39662	6P 12V 10 ºC DTB	AT5G04240.1	*ELF6*	GLM	Q-Matrix
Bo1g011280.1:786:A	C01	A/T/W	6.0844894	0.44220	10P 12V 5 ºC DTF	AT4G31490.1	Coatomer, beta subunit	GLM	Q-Matrix
Bo7g026810.1:124:G	C07	A/G/R	4.7781947	0.36476	6P 12V 10 ºC DTF	AT2G05790.1	O-Glycosyl hydrolases family 17 protein	GLM	PCA
Bo7g104810.1:204:T	C07	A/T/W	5.9788107	0.41678	10P 6V 15 - 5 ºC DTB	AT3G55512	mir172D	GLM	Q-Matrix
Bo2g009460.1:894:T	C02	C/T	7.6880767	0.40565	10P 6V 5 ºC DTF - DTB	AT5G10140.4	*FLC.C2*	GLM	Q-Matrix

Table1